Disorder effects on superconducting tendencies in the checkerboard Hubbard model

Peter M. Smith and Malcolm P. Kennett
Physics Department, Simon Fraser University, 8888 University Drive, Burnaby, British Columbia, Canada V5A 1S6
(Received 22 July 2013; revised manuscript received 12 December 2013; published 31 December 2013)

The question of whether spatially inhomogeneous hopping in the two dimensional Hubbard model can lead to enhancement of superconductivity has been tackled by a number of authors in the context of the checkerboard Hubbard model (CHM). We address the effects of disorder on superconducting properties of the CHM by using exact diagonalization calculations for both potential and hopping disorder. We characterize the superconducting tendencies of the model by focusing on the pair-binding energy, the spin gap, and d-wave pairing order parameter. We find that superconducting tendencies, particularly the pair-binding energy, are more robust to disorder when there is inhomogeneous hopping than for the uniform Hubbard model. We also study all possible staggered potentials for an eight-site CHM cluster and relate the behavior of these configurations to the disordered system.

DOI: 10.1103/PhysRevB.88.214518 PACS number(s): 71.10.Fd, 74.62.En, 74.81.−g, 74.20.Rp

I. INTRODUCTION

The problem of high temperature superconductivity (HTS) in cuprate materials has been at the forefront of condensed matter research since its discovery over 25 years ago.[1] Despite the overwhelming theoretical and experimental efforts focused towards this topic, the microscopic origin of HTS remains elusive. From the theoretical side, the doped two dimensional Hubbard model has been central to many attempts to understand HTS.[2,3] Recent numerical simulations of this model appear to confirm that it can support d-wave superconductivity.[4] Nevertheless, variants of this model are appealing to study as they may allow for further insights into the two dimensional Hubbard model. One such variant that has received much recent attention is the checkerboard Hubbard model (CHM),[5–11] in which hopping on the two dimensional lattice is spatially modulated in a checkerboard pattern.[12–16] This modulation can be tuned to interpolate between the limit of isolated plaquettes and the limit of the uniform two dimensional Hubbard model. The isolated plaquette limit is exactly solvable since it is possible to write down the wave functions and energies as a function of electron number, Hubbard U, and intraplaquette hopping parameter t for a four site Hubbard model.[17] As interplaquette hopping t' is turned on but $t'/t \ll 1$, one can view the CHM as weakly coupled plaquettes and a perturbative approach can be developed.[5] Additional motivation for studying Hubbard models with modulated hopping comes from the evidence for spatial modulations of electronic properties in underdoped cuprate materials[18–20] and proposals for realizing checkerboard fermionic Hubbard models in cold atom systems.[21–24]

Particularly in the context of cuprates, there has been much discussion as to whether inhomogeneity in hopping can enhance superconductivity or not. Kivelson and collaborators[5–7,25,26] have argued that there is an optimal inhomogeneity in the hopping for superconductivity in the Hubbard model based on analytic calculations and exact diagonalization studies.[6] Work using contractor renormalization methods supports this claim.[9] However, calculations using quantum Monte Carlo (QMC) by Doluweera *et al.*[10] and cluster dynamical mean field theory (DMFT) by Chakraborty *et al.*[11] suggest that hopping inhomogeneity may enhance superconductivity for some interaction strengths and dopings, but at others it does not.

Previous studies of the checkerboard Hubbard model have not included disorder, and in this paper we study the effect of disorder on the superconducting properties of the CHM using exact diagonalization calculations. Our motivations for including disorder in the CHM are twofold. First, as mentioned above, when $t'/t = 0$, the model is exactly solvable and so, in this limit, one is able to add disorder to an interacting state that is known exactly, in contrast to the usual Hubbard model ($t'/t = 1$). Second, in Ref. 6 exact diagonalization calculations performed on the CHM were used to argue for an optimal inhomogeneity for superconductivity–if this result is relevant to experimental systems, then it is useful to have understanding of the effects of disorder. We study the effects of both weak and strong potential and hopping disorder on three proxies for superconducting order: the pair-binding energy (PBE), Δ_p, the spin gap, Δ_s, and a d-wave order parameter, Ψ_d. The pair-binding energy is a measure of the tendency towards pairing of hole excitations. The spin gap is the gap between the lowest energy $S = 0$ state and the lowest energy $S = 1$ state. Numerical studies of the homogeneous two-dimensional Hubbard model[4,27–29] using the dynamical cluster approximation (DCA) and quantum Monte Carlo (QMC) simulations have suggested that $S = 1$ particle-hole spin fluctuations act to mediate d-wave pairing. However, neither the PBE nor the spin gap give information about the symmetry of the ground state. Hence we also calculate a d-wave order parameter, which has been investigated by several authors, to obtain insight into the ground state symmetry of the CHM.[6,11] Although potential disorder is a pair-breaking perturbation for d-wave superconductors,[30] a recent numerical study of the uniform Hubbard model suggested that very weak potential disorder can enhance antiferromagnetic spin correlations and lead to a small increase in the critical temperature.[27]

We study eight- and twelve-site systems at dopings $x = 1/8$ and $x = 1/12$, respectively, for both potential and hopping disorder over a wide range of disorder strengths. Our results in the weak disorder limit are similar to previous exact diagonalization studies: we find that superconducting tendencies are enhanced for intermediate hopping inhomogeneity, with the tendency most pronounced in the PBE and the spin gap. We also find that with increasing disorder, superconducting

tendencies are most robust to disorder in the region of intermediate hopping inhomogeneity, which is our main result. We note that potential disorder can be considered as a random linear combination of specific staggered potentials, although the resulting electronic properties are not a simple linear combination of the properties for each potential configuration. For eight-site clusters, it is straightforward to enumerate all inequivalent staggered potentials and we study the effects of each of these potentials on the pair-binding energy, the spin gap, and the d-wave order parameter.

This paper is organized as follows. In Sec. II, we introduce the disordered checkerboard Hubbard model and define the quantities we calculate. In Sec. III, we show the results of our finite diagonalization studies of eight- and twelve-site clusters and discuss how disorder averaging affects the properties of the PBE (Sec. III A), the spin gap (Sec. III B), and the d-wave pairing order parameter (Sec. III C). In Sec. IV we discuss the effects of introducing staggered potential disorder on these quantities for an eight-site system. We conclude and discuss our results in Sec. V.

II. MODEL AND QUANTITIES CALCULATED

In this section, we define the checkerboard Hubbard model, specify the different types of disorder we consider, and define the quantities we calculate: the pair-binding energy, the spin gap, and the d-wave order parameter. The disordered CHM consists of N electrons on an M site lattice with a Hubbard-Anderson Hamiltonian,

$$H = -\sum_{ij} t_{ij}(\hat{c}^{\dagger}_{i\sigma}\hat{c}_{j\sigma} + \text{H.c.}) + \sum_{i} U_i \hat{n}_{i\uparrow}\hat{n}_{i\downarrow} + \sum_{i\sigma} W_i \hat{n}_{i\sigma}, \tag{1}$$

where $\hat{c}^{\dagger}_{i\sigma}$ is a fermionic creation operator for a spin-σ electron on site i, $\hat{n}_{i\sigma} = \hat{c}^{\dagger}_{i\sigma}\hat{c}_{i\sigma}$ is the number operator, t_{ij} is a hopping amplitude, U_i is an on-site Hubbard interaction, and W_i is an on-site disorder potential. We choose $U_i = U$ on all sites of the lattice and $W_i = W\delta_i$, where δ_i is drawn with uniform probability from $[-0.5,0.5]$. We focus on the situation in which the hopping parameters define a checkerboard,[5,6] as illustrated in Fig. 1:

$$t_{ij} = \begin{cases} t, & \langle ij\rangle \in I, \\ t', & \langle ij\rangle, i \in I, j \in J, I \neq J, \\ 0, & \text{otherwise.} \end{cases}$$

Lowercase letters (ij) label sites on the lattice, uppercase letters (IJ) label plaquettes, and $\langle ij\rangle$ indicates that sites i and j are nearest neighbors on the lattice. Thus t gives the magnitude of the hopping term on a single plaquette, while t' gives the magnitude of interplaquette hopping. Without loss of generality, we choose $t' \leqslant t$.

We consider two types of disorder: on-site potential disorder, as discussed above, and hopping disorder, corresponding to disorder in the intraplaquette ($t_{ij} = t$) nearest neighbor hopping terms. For sites i and j on plaquette I, we choose $t_{ij} = t[1 + \eta_{ij}(W/t)]$, where η_{ij} is drawn with uniform probability from $[-0.5,0.5]$. For random hopping we always consider $W < 2$, so that the t_{ij} are always positive.

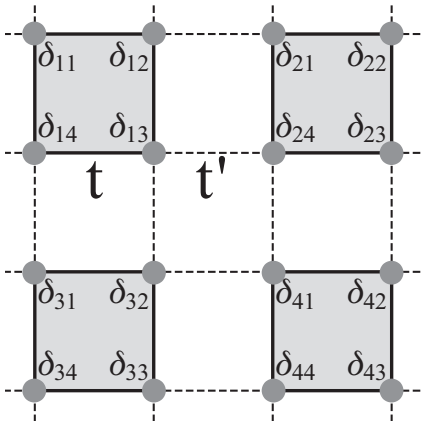

FIG. 1. Illustration of the inhomogeneous hopping terms t and t' and the distribution of disorder in the checkerboard Hubbard model with potential disorder. δ_{Ab} is the disorder potential on site b of plaquette A.

A. Pair-binding energy

Let E_m be the ground state energy of an M site cluster with m holes, where $m \geqslant 1$ and is measured from half-filling. The pair-binding energy (PBE) for that M-site cluster is

$$\Delta_p = 2E_m - (E_{m+1} + E_{m-1}). \tag{2}$$

The PBE can be interpreted physically in the following way: for a system of two identical clusters with an average of m holes per cluster, $\Delta_p > 0$ indicates that it is energetically favorable to place $m+1$ holes on one cluster and $m-1$ holes on the other, rather than m holes on both clusters.

To study the role of disorder on the pair-binding properties of the inhomogeneous Hubbard model, we study both the disorder-averaged pair-binding energy and the distribution of pair-binding energies as functions of U/t, t'/t, and W/t. For a specific disorder configuration k, we define the associated PBE to be

$$\Delta^k_p = 2E^k_m - \left(E^k_{m+1} + E^k_{m-1}\right),$$

where E^k_m is the ground state energy of disorder configuration k when it has m holes. The disorder-averaged PBE is

$$\langle\Delta_p\rangle = \frac{1}{K}\sum_{k=1}^{K}\Delta^k_p, \tag{3}$$

where the angle brackets $\langle\cdots\rangle$ indicate an average over K disorder configurations and it is understood that $\langle\Delta_p\rangle$ is a function of U/t, W/t, and t'/t. We also calculate the probability of measuring a positive PBE for any given disorder configuration by averaging over K configurations at fixed W. We denote this quantity by $P(\Delta^k_p > 0)$.

B. Spin gap

Let $E_0(m = 2, S = 0)$ and $E_0(m = 2, S = 1)$ denote the energies of the lowest-lying $S = 0$ state and the lowest-lying $S = 1$ state of two holes, respectively. The spin

gap,

$$\Delta_s = E_0(m = 2, S = 1) - E_0(m = 2, S = 0), \quad (4)$$

also provides a measure of the energy scale towards pairing in the CHM. In BCS theory, in the thermodynamic limit,

$$\lim_{N\to\infty} \Delta_s = \lim_{N\to\infty} \Delta_p = 2\Delta_0,$$

where N is the system size and Δ_0 is the superconducting gap.[25] We calculate the disorder-averaged spin gap,

$$\langle \Delta_s \rangle = \frac{1}{K} \sum_{k=1}^{K} \Delta_s^k, \quad (5)$$

and study how it behaves as a function of disorder strength.

In the absence of disorder, the total spin eigenvalue of the $m = 2$ ground state is $S = 0$ for all t'/t and U/t not too large ($U/t \lesssim 20$). The introduction of disorder alters the energy spectrum, which may lead to level crossings between $S = 0$ states and $S = 1$ states depending on the strength of interactions, intraplaquette hopping, and disorder strength. Hence we also calculate the probability of finding $S = 1$ in the ground state of the $m = 2$ system for each cluster size as a function of U/t, t'/t, and W/t.

C. d-wave pairing order parameter

The PBE and the spin gap provide measures of the tendency towards superconductivity in the CHM. However, neither of these quantities give information about the symmetry of the ground state in the region of parameter space where these quantities are positive. It is expected[5–11,25] that superconductivity in the CHM has d-wave symmetry; hence we calculate a d-wave order parameter of a standard form.[30] Let $\hat{D}$ be the singlet operator acting on the bonds, defined by

$$\hat{D} = \sum_{\langle ij \rangle} D_{ij} c_{i\uparrow} c_{j\downarrow}, \quad (6)$$

where D_{ij} is equal to $+1$ on bonds oriented along the x direction and -1 for bonds along the y direction. The disorder-averaged d-wave order parameter is then the matrix element between ground states with m and $m - 2$ holes:

$$\langle \Psi_d \rangle = \frac{1}{K} \sum_{k=1}^{K} \langle S = 0, m; k | \hat{D} | S = 0, m - 2; k \rangle. \quad (7)$$

III. EXACT DIAGONALIZATION RESULTS

We now discuss the results obtained from exact diagonalization of the disordered CHM in the presence of on-site and hopping disorder on eight- and twelve-site clusters. We consider the ladder geometries shown in Fig. 2 for eight- and twelve-site clusters. The boundary conditions are periodic along the direction of the length of the ladder for ladder geometries. We study the dopings $x = 1/8$ for eight-site clusters and $x = 1/12$ for twelve-site clusters. We calculate all quantities discussed in Sec. II as a function of increasing disorder strength and compare our results to the clean system. We measure all energies in units of t. For each type of disorder, we average over 256 disorder realizations for eight-site clusters and 64 disorder realizations for twelve-site clusters.

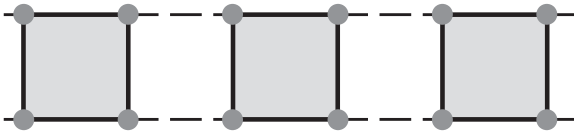

FIG. 2. Lattice geometry studied in this paper, shown for 12 sites.

The data presented in this paper focused primarily on exact diagonalization of ladder systems. Tsai *et al.*[5,6] performed exact diagonalization calculations for the sixteen-site lattice at doping $x = 1/16$ and $3/16$ and found evidence for an optimal value of inhomogeneity in the CHM. Tsai *et al.* were able to make use of a number of symmetries to simplify their exact diagonalization calculations. As soon as disorder is introduced, all real-space symmetries of the lattice are lost immediately, which means that it is harder to solve sixteen-site systems, and makes calculating the disorder-averaged spin gap and d-wave order parameter much more difficult. We have hence mainly focused on obtaining disorder-averaged results for eight- and twelve-site lattices.

Convergence to the extremal eigenvalues is rapid when using the Lanczos method, so that ground state energies (required for the pair-binding energy) can be calculated to machine precision. Our results for the pair-binding energy match up well with those of other studies.[31] In addition to calculating the ground state energy, we calculate the associated eigenvector (which is required for calculation of the d-wave order parameter) using the restarted Lanczos method. For quantities such as the spin gap, excited states are required. To calculate the first excited state, we restart the Lanczos algorithm with the constraint that all Lanczos vectors are orthogonal to the ground state. Once the convergence criterion is met, we verify that the calculated state is orthogonal to the ground state. This scheme allows us to calculate the ground state and the first few excited states as a function of system parameters.

A. Pair-binding energy

Numerical studies of the CHM employing dynamical cluster QMC[10] and cluster DMFT[11] suggest that d-wave superconductivity is generally suppressed relative to the homogeneous case by introducing inhomogeneity in hopping. These studies suggest that the maximum values of either T_c or the d-wave order parameter generally do not exceed that of the homogeneous system. On the other hand, results from exact diagonalization studies of the CHM on 4×4 lattices[5,6] and DMRG studies of the CHM on ladders[25] suggest that at low doping the CHM can have enhanced d-wave pairing compared to the uniform Hubbard model. In Refs. 5, 6, and 25, the optimal parameters that maximize the PBE are $t' = 0.5t$ and $U = 8t$ for a 4×4 system at doping $x = 1/16$ and $t' \approx 0.6$–$0.8t$ and $U = 6t$ in a ladder system at doping $x = 1/8$. Moreover, these results indicate that other quantities relevant to superconductivity, such as the spin gap, d-wave pairing operator, and pair-field correlations, are also optimized in the region where the PBE is maximal. Thus the PBE should be a reasonable measure for predicting where in parameter

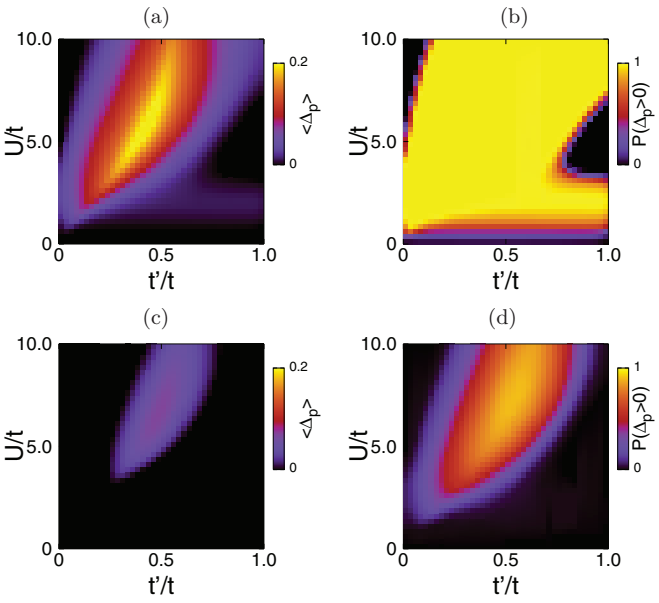

FIG. 3. (Color online) Disorder-averaged pair-binding energy, $\langle\Delta_p\rangle$, and the probability of observing a positive pair-binding energy, $P(\Delta_p^k > 0)$, for the eight-site ladder at doping $x = 1/8$ with potential disorder: (a) $\langle\Delta_p\rangle, W/t = 0.05$; (b) $P(\Delta_p^k > 0), W/t = 0.05$; (c) $\langle\Delta_p\rangle, W/t = 1.00$; (d) $P(\Delta_p^k > 0), W/t = 1.00$.

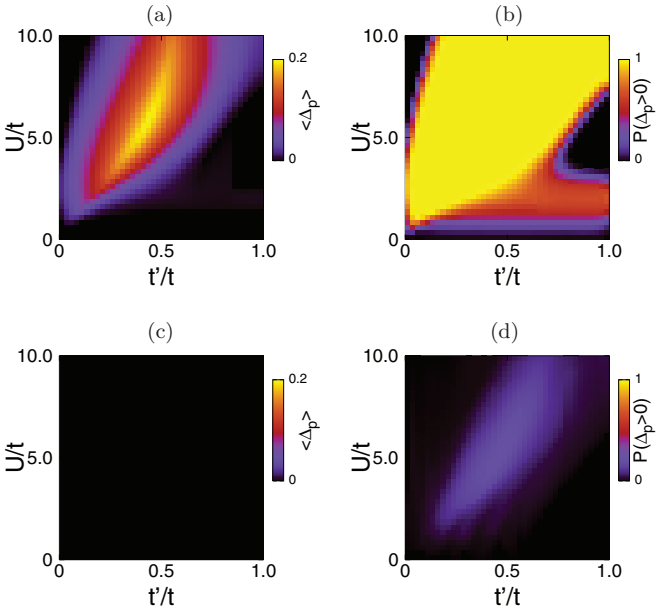

FIG. 4. (Color online) Disorder-averaged pair-binding energy, $\langle\Delta_p\rangle$, and the probability of observing a positive pair-binding energy, $P(\Delta_p^k > 0)$, for the eight-site ladder at doping $x = 1/8$ with hopping disorder: (a) $\langle\Delta_p\rangle, W/t = 0.05$; (b) $P(\Delta_p^k > 0), W/t = 0.05$; (c) $\langle\Delta_p\rangle, W/t = 1.00$; (d) $P(\Delta_p^k > 0), W/t = 1.00$.

space the tendency towards superconductivity in the CHM may be strongest.

Previous work on the superconducting properties of the CHM was in the clean limit.[5,6,10,11,25] Here, we ask how disorder affects these properties. We determine the degree to which disorder enhances or suppresses d-wave superconductivity in such systems. In Figs. 3–6, we plot $\langle\Delta_p\rangle$ and $P(\Delta_p^k > 0)$ as functions of t'/t and U/t at $W/t = 0.05$ [Fig. (a)] and $W/t = 1.00$ [Fig. (c)] for the eight-site ladder and twelve-site ladder geometries for potential and hopping disorder. In order to see the regions where pair binding is favored as disorder is increased, we plot only the values $\langle\Delta_p\rangle > 0$. For both types of disorder, there exists an intermediate range of parameters t'/t and U/t where pair binding is enhanced relative to the standard Hubbard model ($t'/t = 1$).

For the eight-site ladder, at weak disorder, we find that $\langle\Delta_p\rangle$ appears to be maximum near $t'/t \approx 0.42$ at $U/t \approx 5.6$ for $x = 1/8$. For the twelve-site ladder, at weak disorder, the optimal parameters are qualitatively similar, as $\langle\Delta_p\rangle$ is maximal near $t'/t \approx 0.4$ and $U/t \approx 5.0$ for $x = 1/12$. This is similar to the results of Tsai *et al.*,[5,6] who found the pair-binding energy to be maximal at $U/t \approx 8$ and $t'/t \approx 0.5$ for doping $x = 1/16$ on a sixteen-site cluster.

We find the maximum value of $\langle\Delta_p\rangle$ is always less than the maximum value of the PBE in the absence of disorder. As disorder strength is increased, the maximum value of $\langle\Delta_p\rangle$ decreases. Furthermore, the region in $t' - U$ parameter space where $\langle\Delta_p\rangle > 0$ shrinks as W/t is increased, with the greatest persistence in the region of maximum PBE in the absence of disorder. For the eight-site ladder, we find that $\langle\Delta_p\rangle$ becomes negative at $W/t \approx 1.50$ for all t'/t and U/t studied for on-site disorder and $W/t \approx 1.00$ for hopping disorder, with similar cutoff values for the twelve-site ladders. For weak disorder, the pair-binding properties of the system in the region of maximum $\langle\Delta_p\rangle$ are qualitatively unchanged in the case of either on-site disorder or hopping disorder. The range in $t' - U$ space where there is a nonzero probability that pair binding is favored for some disorder configurations is much wider than the region

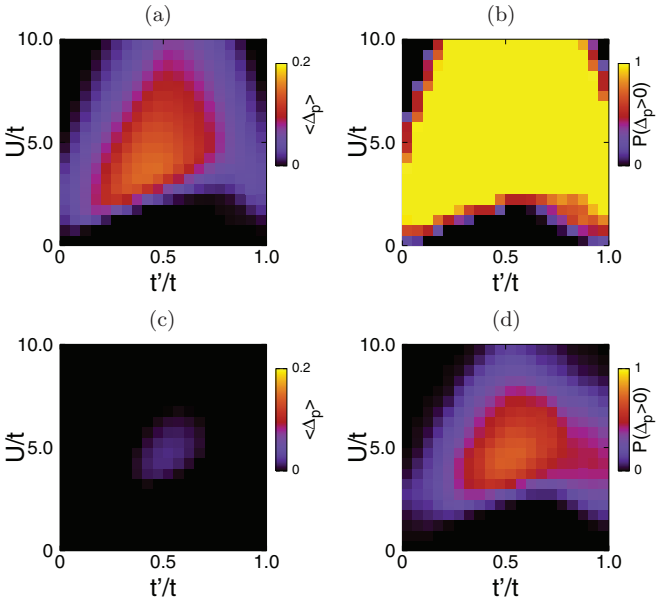

FIG. 5. (Color online) Disorder-averaged pair-binding energy, $\langle\Delta_p\rangle$, and the probability of observing a positive pair-binding energy, $P(\Delta_p^k > 0)$, for the twelve-site ladder at doping $x = 1/12$ with potential disorder: (a) $\langle\Delta_p\rangle, W/t = 0.05$; (b) $P(\Delta_p^k > 0), W/t = 0.05$; (c) $\langle\Delta_p\rangle, W/t = 1.00$; (d) $P(\Delta_p^k > 0), W/t = 1.00$.

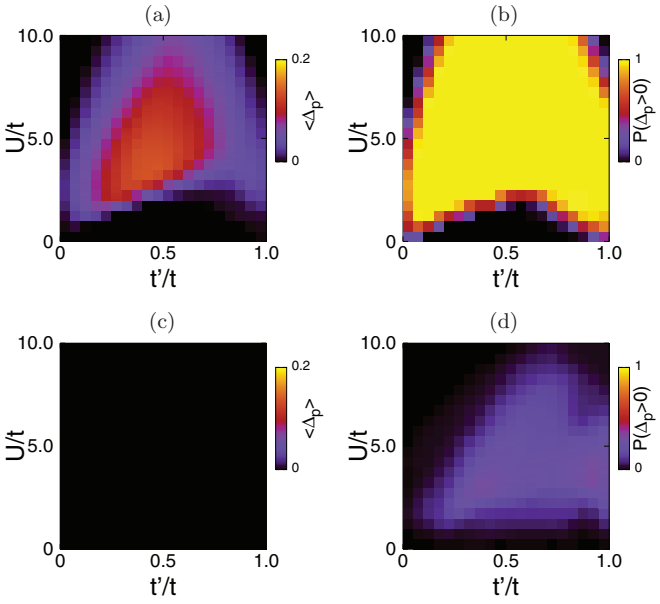

FIG. 6. (Color online) Disorder-averaged pair-binding energy, $\langle\Delta_p\rangle$, and the probability of observing a positive pair-binding energy, $P(\Delta_p^k > 0)$, for the twelve-site ladder at doping $x = 1/12$ with hopping disorder: (a) $\langle\Delta_p\rangle, W/t = 0.05$; (b) $P(\Delta_p^k > 0), W/t = 0.05$; (c) $\langle\Delta_p\rangle, W/t = 1.00$; (d) $P(\Delta_p^k > 0), W/t = 1.00$.

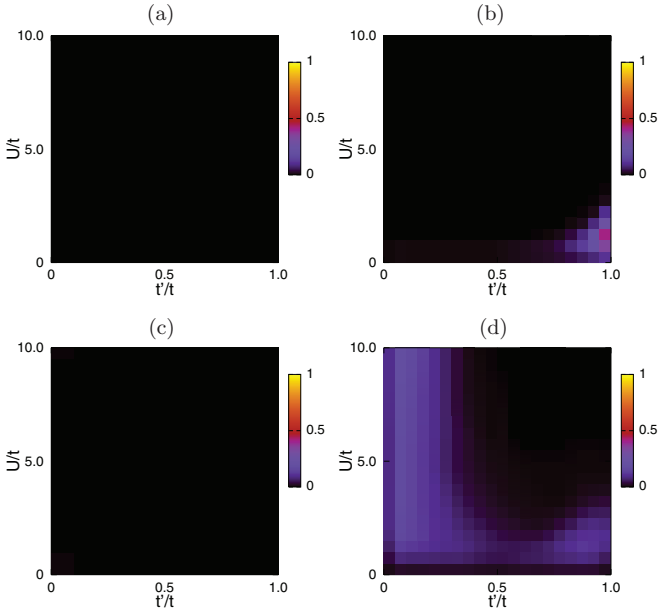

FIG. 7. (Color online) Probability of observing a $S = 1$ ground state in the $m = 2$-hole doped system, $P(S = 1)$, for the eight-site ladder cluster at doping $x = 1/8$: (a) potential disorder, $W/t = 0.05$; (b) potential disorder, $W/t = 1.00$; (c) hopping disorder, $W/t = 0.05$; (d) hopping disorder, $W/t = 1.00$.

where pair binding is favored on average and persists to much higher values of W/t.

If one interprets the PBE as a measure of the tendency of the system to become superconducting, then our results can be interpreted in the following way: as disorder is increased, the region in parameter space where pair binding is favoured *on average* decreases, consistent with finite disorder suppressing superconductivity. However, the fact that $P(\Delta_p^k > 0) \neq 0$ even when $\langle\Delta_p\rangle < 0$ suggests that there are local regions in real space where superconductivity can persist even when it is suppressed on average. Our results also suggest that pair binding in the CHM is more robust to disorder than in the uniform Hubbard model as W/t increases. As disorder is increased, $\langle\Delta_p\rangle$ is suppressed rapidly near $t'/t = 1$, while pair binding persists at intermediate values of inhomogeneity for large values of W/t.

We also find that disorder affects the spin eigenvalue of the ground state. In Figs. 7 and 8 we plot the probability of finding $S = 1$ eigenvalues in the $m = 2$-hole ground state, $P(S = 1)$, for the eight- and twelve-site ladder clusters. We find that the ground state of the eight-site ladder always has $S = 0$ for weak disorder. However, at $W/t = 1$, $P(S = 1)$ appears to be maximum at $t'/t = 1$ and $U/t \approx 2$, which corresponds to the maximum of the PBE of the uniform, homogeneous eight-site ladder cluster. In the twelve-site ladder cluster, there is a region with $0.4 \lesssim t'/t \lesssim 0.8$ for $U/t < 3$ where the ground state is mainly $S = 1$ even for weak disorder. As disorder strength increases, the value of $P(S = 1)$ decreases in this region while simultaneously increasing around $t'/t \approx 0$ and $t'/t \approx 1$. At $W/t = 1$, $P(S = 1) = 0$ for intermediate values of t'/t and $U/t > 5$ for both the eight- and twelve-site ladder clusters.

For both eight- and twelve-site clusters, the region in parameter space where $P(S = 1) > 0$ is larger for hopping disorder than for potential disorder as disorder strength increases. In both cases, at weak disorder the largest values of $P(S = 1)$ are found for intermediate t'/t and $U/t \lesssim 3$. From the definition of the d-wave order parameter, when the total spin of the ground state is $S = 1$, $\Psi_d = 0$. We expect $\langle\Psi_d\rangle$ to

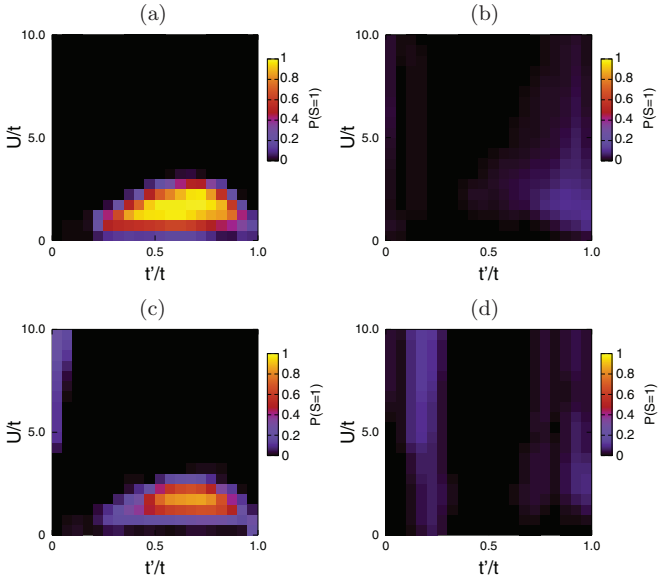

FIG. 8. (Color online) Probability of observing a $S = 1$ ground state in the $m = 2$-hole doped system, $P(S = 1)$, for the twelve-site ladder cluster at doping $x = 1/12$: (a) potential disorder, $W/t = 0.05$; (b) potential disorder, $W/t = 1.00$; (c) hopping disorder, $W/t = 0.05$; (d) hopping disorder, $W/t = 1.00$.

be most robust against potential disorder in the regions where $P(S=1)=0$ up to $W/t=1$.

B. Spin gap

Karakonstantakis *et al.*[25] calculated the spin gap and the PBE in the ladder CHM using density matrix renormalization group (DMRG) methods and argued that there is an optimal inhomogeneity that leads to maximal values of Δ_p and Δ_s. Similar to Ref. 25, we calculate the disorder-averaged spin gap, $\langle\Delta_s\rangle$, as the average gap between the $S=0$ state and the lowest-energy $S=1$ state in the $m=2$-hole doped system. The spin gap, like the pair-binding energy, may be interpreted as a measure of the pairing scale of the system.[29]

In order to evaluate the spin gap, we calculate the eigenvalues and associated eigenvectors of the ground state and the first few excited states, determine the S^2 eigenvalue of each state, isolate the lowest-lying $S=1$ eigenstate, and then calculate $E_0(S=1)-E_0(S=0)$. There also exist several low-lying states with $S=0$ near the $S=1$ state, and for large enough t'/t, we see crossings between the lowest-lying $S=1$ state and $S=0$ excited states. We plot $\langle\Delta_s\rangle$ as a function of t'/t and U/t at fixed W/t for the eight-site ladder, but focus on $U/t=8.0$ for the twelve-site ladder. The reason for the latter situation is that there are multiple level crossings between excited states in the twelve-site model, which makes it difficult to survey numerically the spectrum of excited states for many values of t'/t and U/t. We also calculate the disorder-averaged gap between the ground state and the first excited $S=0$ state, $\langle E_1-E_0\rangle$, to get a better sense of how the lowest-lying $S=0$ states behave as t'/t is varied. The value of $\langle E_1-E_0\rangle$ is calculated only for those configurations where the ground state has $S=0$.

We plot $\langle\Delta_s\rangle$ and $\langle E_1-E_0\rangle$ for the eight- and twelve-site ladders in Figs. 9–14. For eight-site clusters with weak disorder and moderate interactions, the spin gap increases monotonically as $t'/t\to 1$. As disorder increases, the gap appears to soften slightly as $t'/t\to 1$, which leads to the optimal $\langle\Delta_s\rangle$ occurring for $t'/t<1$, albeit with different U/t and t'/t to where pair binding is favored. On the other hand, the results for $\langle E_1-E_0\rangle$ for eight-site clusters show that this quantity is maximized for intermediate values of inhomogeneity. Also of interest is that for $t'/t\gtrsim 0.7$, $\langle E_1-E_0\rangle<\langle\Delta_s\rangle$, indicating that the lowest-lying excitations are $S=0$ states. However, there is a maximum in $\langle E_1-E_0\rangle$ at $t'/t\approx 0.5$ for which $\langle E_1-E_0\rangle>\langle\Delta_s\rangle$. As $t'/t\to 1$, we find $\langle E_1-E_0\rangle<\langle\Delta_s\rangle$.

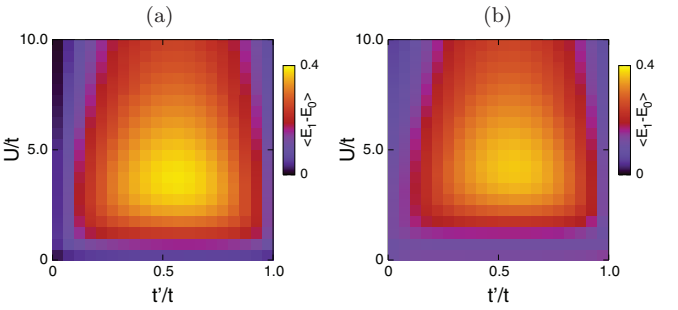

FIG. 10. (Color online) Disorder-averaged gap to the lowest energy $S=0$ excited state, $\langle E_1-E_0\rangle$, as a function of t'/t and U/t at doping $x=1/8$ on the eight-site ladder with potential disorder: (a) $W/t=0.05$ and (b) $W/t=1.00$.

At weak disorder in eight-site clusters, the results for $\langle\Delta_p\rangle$ and $\langle E_1-E_0\rangle$ show little qualitative difference between potential and hopping disorder. However, we see a clear difference between both types of disorder at large W/t. As illustrated in Figs. 11 and 12, for hopping disorder, $\langle\Delta_s\rangle$ and $\langle E_1-E_0\rangle$ grow with increasing W/t, whereas for potential disorder large values of W/t appear to suppress these quantities slightly.

For twelve-site ladder clusters with $U/t=8$, $\langle\Delta_s\rangle$ appears to be maximized at $t'/t\approx 0.5$, while $\langle E_1-E_0\rangle$ appears to be maximized at $t'/t\approx 0.4$. A comparison between this result and the data for the spin gap calculated on eight-site clusters, which show no signs of "optimization" for intermediate t'/t, suggests that doping effects are significant when calculating the spin gap. However, similarly to the eight-site clusters, we see a crossover in the gaps as a function of intraplaquette hopping around $t'/t\approx 0.6$ for weak disorder. Depending on disorder strength and configuration, there may be several $S=0$ states with lower energy than the lowest $S=1$. Although this may be an artifact of small system size and/or geometry, our results still suggest that the spin gap is less than the gap to other low-lying $S=0$ states for $t'/t<0.5$; above this value, other low-lying states may lie below the spin gap. Similarly to the eight-site model, it appears that $\langle\Delta_s\rangle$ is affected more by hopping disorder than by potential disorder, as can be seen in Figs. 11 and 14.

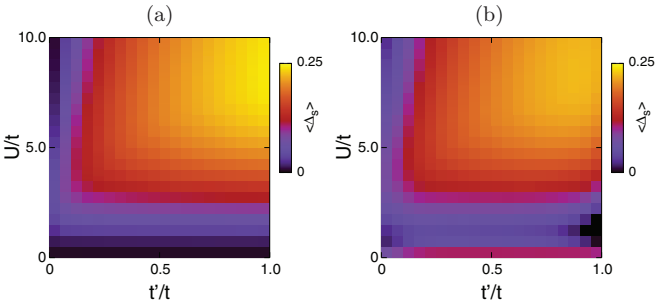

FIG. 9. (Color online) Disorder-averaged spin gap, $\langle\Delta_s\rangle$, as a function of t'/t and U/t at doping $x=1/8$ on the eight-site ladder with potential disorder: (a) $W/t=0.05$ and (b) $W/t=1.00$.

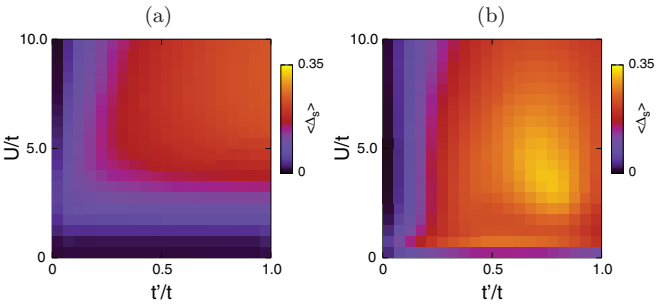

FIG. 11. (Color online) Disorder-averaged spin gap, $\langle\Delta_s\rangle$, as a function of t'/t and U/t at doping $x=1/8$ on the eight-site ladder with hopping disorder: (a) $W/t=0.05$ and (b) $W/t=1.00$.

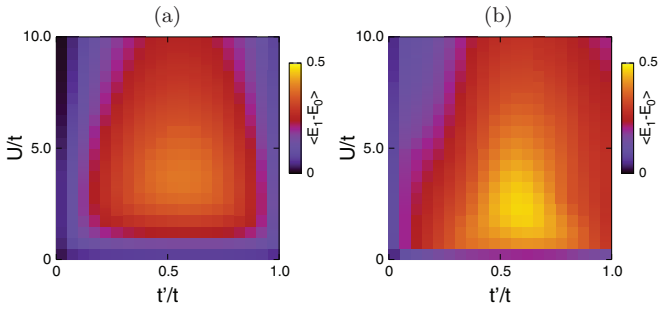

FIG. 12. (Color online) Disorder-averaged gap to the lowest energy $S = 0$ excited state, $\langle E_1 - E_0 \rangle$, as a function of t'/t and U/t at doping $x = 1/8$ for the eight-site ladder with hopping disorder: (a) $W/t = 0.05$ and (b) $W/t = 1.00$.

C. *d*-wave pairing

We investigate d-wave symmetry of the ground state by studying the disorder-averaged d-wave order parameter, $\langle \Psi_d \rangle$. The results for $\langle \Psi_d \rangle$ for the eight- and twelve-site ladder clusters are plotted in Figs. 15–18.

The data for the eight-site and twelve-site ladder clusters show that $\langle \Psi_d \rangle$ is maximized for intermediate values of inhomogeneity, which is consistent with the results for $\langle \Delta_p \rangle$. However, there are some important distinctions between the regions where $\langle \Psi_d \rangle$ and $\langle \Delta_p \rangle$ are strong. First, there is a strong maximum in $\langle \Psi_d \rangle$ near $t'/t \approx 0$ for small U/t as illustrated in Figs. 15 and 16. Furthermore, the data shown in these graphs suggest that $\langle \Psi_d \rangle$ is strongly dependent on the strength and type of disorder in this region of parameter space. Second, $\langle \Psi_d \rangle$ appears to be much more robust against increasing disorder for intermediate values of inhomogeneity than $\langle \Delta_p \rangle$. As such, it appears that disorder does not greatly affect the d-wave symmetry of the ground state as t'/t is increased from zero to unity. We will discuss this second point in more detail in Sec. III D.

Recall from Eqs. (6) and (7) that $\langle \Psi_d \rangle$ has contributions from the strong (t) and weak bonds (t'). Tsai *et al.*[6] showed that for a clean system the contribution to the d-wave order parameter comes strictly from the strong bonds. We find however that the weak bonds contribute to the value of the order parameter for nonzero disorder in the limits of strong and weak inhomogeneity, and this effect is more pronounced for hopping disorder than potential disorder. For intermediate inhomogeneity, the strong bonds make the dominant contributions to the value of the order parameter. These results suggest that the properties of $\langle \Psi_d \rangle$ are more robust against disorder for intermediate to large values of t'/t in comparison to the case of $t'/t \approx 0$ or $t'/t \simeq 1$.

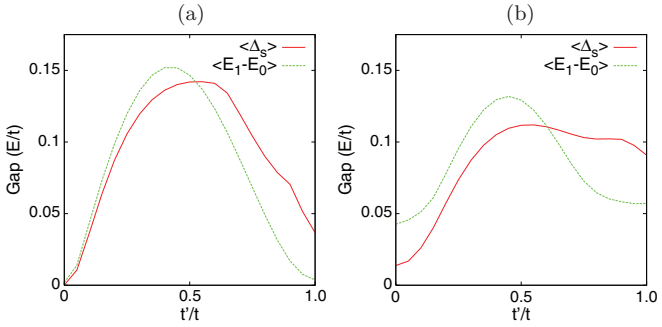

FIG. 13. (Color online) Disorder-averaged spin gap, $\langle \Delta_s \rangle$, and disorder-averaged gap to the lowest energy $S = 0$ excited state, $\langle E_1 - E_0 \rangle$, as a function of t'/t for $U/t = 8$ and doping $x = 1/12$ for the twelve-site ladder with potential disorder: (a) $W/t = 0.05$ and (b) $W/t = 1.00$.

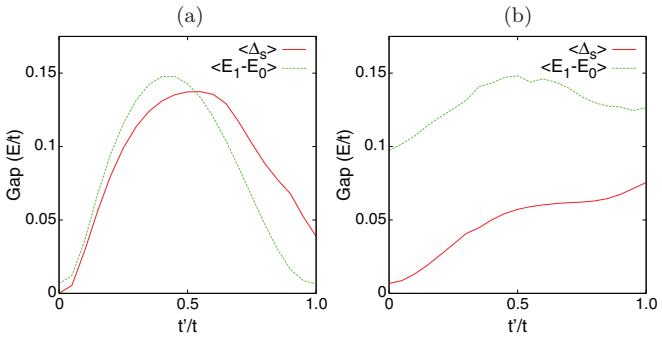

FIG. 14. (Color online) Plots of the disorder-averaged spin gap, $\langle \Delta_s \rangle$, and disorder-averaged gap to the lowest energy $S = 0$ excited state, $\langle E_1 - E_0 \rangle$, as a function of t'/t for $U/t = 8$ and doping $x = 1/12$ for the twelve-site ladder with hopping disorder: (a) $W/t = 0.05$ and (b) $W/t = 1.00$.

The results for $\langle \Delta_p \rangle$ show that as disorder is increased, pair binding is suppressed on average. However, the results for $P(\Delta_p^k > 0)$ suggest that pair binding can still be favored at large W/t for certain configurations even when $\langle \Delta_p \rangle < 0$. We investigate disorder-induced fluctuations of the pair-binding energy by calculating the variance of Δ_p:

D. Disorder-induced fluctuations

$$\sigma_p = \sqrt{\frac{1}{K}\sum_{k=1}^{K}\left(\Delta_p^k - \langle \Delta_p \rangle\right)^2}. \tag{8}$$

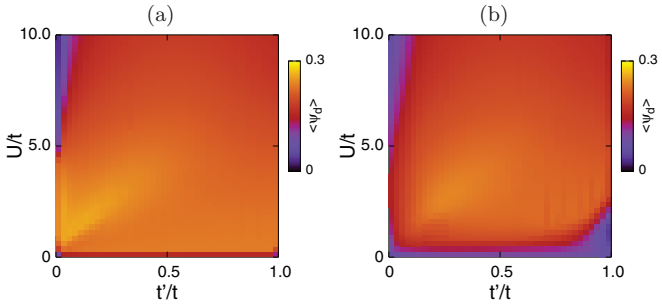

FIG. 15. (Color online) Disorder-averaged d-wave pairing order parameter, $\langle \Psi_d \rangle$, on the eight-site ladder with potential disorder: (a) $W/t = 0.05$ and (b) $W/t = 1.00$.

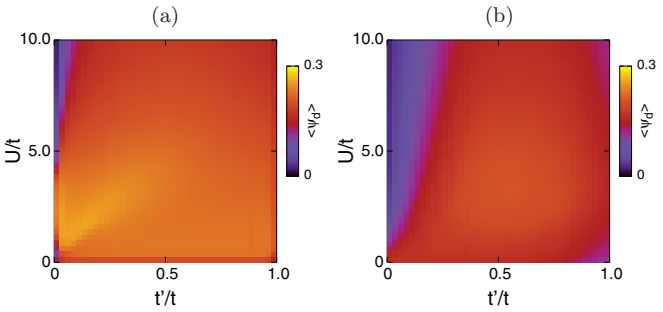

FIG. 16. (Color online) Disorder-averaged d-wave pairing order parameter, $\langle \Psi_d \rangle$, on the eight-site ladder with hopping disorder: (a) $W/t = 0.05$ and (b) $W/t = 1.00$.

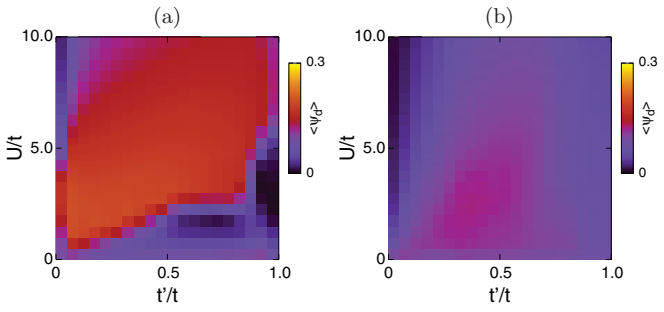

FIG. 18. (Color online) Disorder-averaged d-wave pairing order parameter, $\langle \Psi_d \rangle$, on the twelve-site ladder with hopping disorder: (a) $W/t = 0.05$ and (b) $W/t = 1.00$. The black regions in (a) correspond to $P(S = 1) \approx 1$.

In Figs. 19 and 20 we plot $\log(\sigma_p)$ to illustrate the magnitude of the disorder-induced fluctuations. At weak disorder, $\log(\sigma_p)$ shows a clear minimum in the region of maximum $\langle \Delta_p \rangle$ for both potential and hopping disorder.

This minimum has the form of a cusp, although it is smoothed out with increasing disorder strength. The cusp is more pronounced for twelve-site clusters: for $t'/t < (t'/t)_{\text{optimal}}$, the value of σ_p decreases by almost an order of magnitude from its value at $t'/t = 0.5$ at weak disorder, illustrating the change in the distribution of pair-binding energies from $t'/t < (t'/t)_{\text{optimal}}$ to $t'/t > (t'/t)_{\text{optimal}}$. One possible explanation is that the location of the cusp signals a crossover from isolated plaquette physics to inhomogeneous lattice physics. This is similar to the transition observed by Peterson *et al.*[21] in the case of the d-Mott insulator state.

We have also investigated fluctuations in the spin gap and the d-wave order parameters. In each case, the fluctuations are weakest in the region where the disorder-averaged quantities are maximal. Unlike σ_p, disorder-induced fluctuations in the spin gap and the d-wave order parameter do not exhibit any cusplike features.

IV. STAGGERED POTENTIALS

One way of viewing a particular disorder configuration in either potential or hopping strength is as a linear combination of staggered on-site potential or hopping configurations, where the deviation from a uniform system on each site or bond can only take values of $\pm\frac{W}{2}$. On an eight-site ladder cluster, with periodic boundary conditions along the ladder, there are 32 possible nontrivial inequivalent staggered configurations for either potentials or hoppings. Even though for an interacting problem we cannot take a linear combination of solutions for different potentials to determine the full behavior, studying individual staggered potentials can lead to insights into their contributions in random potentials. Hence we study Δ_p, Δ_s, and Ψ_d at doping $x = 1/8$ for all staggered on-site potentials and hopping patterns.

In Figs. 21(a) and 21(b) we plot the maximum Δ_p in the $U - t'$ plane for all 32 staggered potential and hopping configurations for several different values of disorder strength. For most configurations the maximum value of Δ_p is suppressed as $W/t \to 1$. However, as disorder strength is increased beyond this limit, there are some configurations where pair binding persists to large W/t. This is in contrast to the behavior of

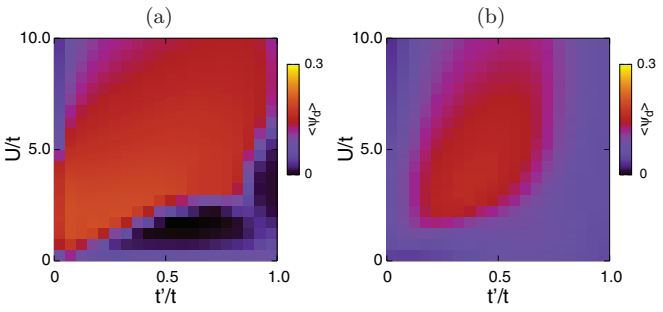

FIG. 17. (Color online) Disorder-averaged d-wave pairing order parameter, $\langle \Psi_d \rangle$, on the twelve-site ladder with potential disorder: (a) $W/t = 0.05$ and (b) $W/t = 1.00$. The black regions in (a) correspond to $P(S = 1) \approx 1$.

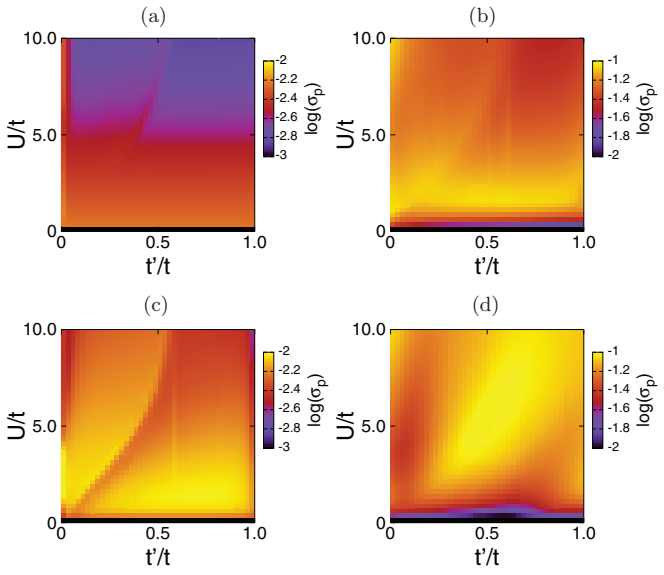

FIG. 19. (Color online) Plots of $\log(\sigma_p)$ for the eight-site ladder cluster at doping $x = 1/8$: (a) potential disorder, $W/t = 0.05$; (b) potential disorder, $W/t = 1.00$; (c) hopping disorder, $W/t = 0.05$; (d) hopping disorder, $W/t = 1.00$.

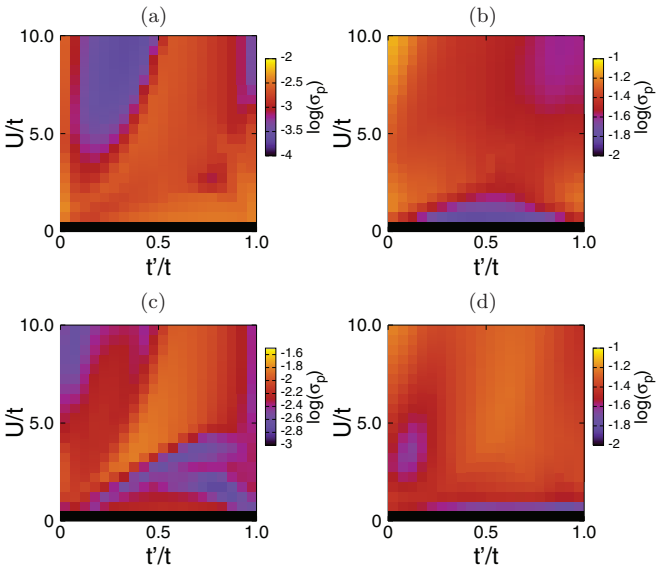

FIG. 20. (Color online) Plots of $\log(\sigma_p)$ for the twelve-site ladder cluster at doping $x = 1/12$: (a) potential disorder, $W/t = 0.05$; (b) potential disorder, $W/t = 1.00$; (c) hopping disorder, $W/t = 0.05$; (d) hopping disorder, $W/t = 1.00$.

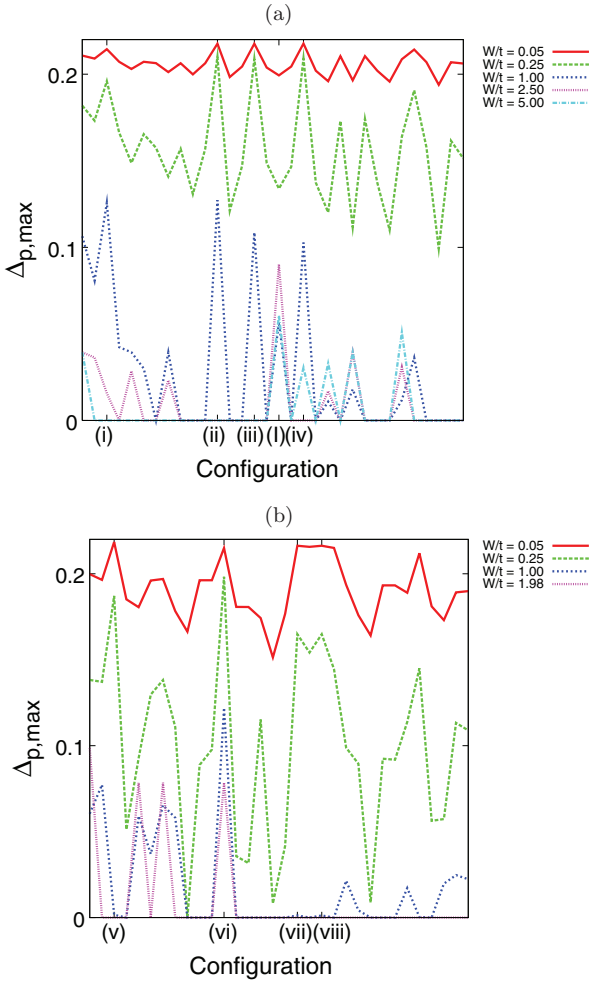

FIG. 21. (Color online) Plots of $\Delta_{p,\max}$ for each staggered configuration as a function of W/t: (a) staggered potentials; (b) staggered hopping.

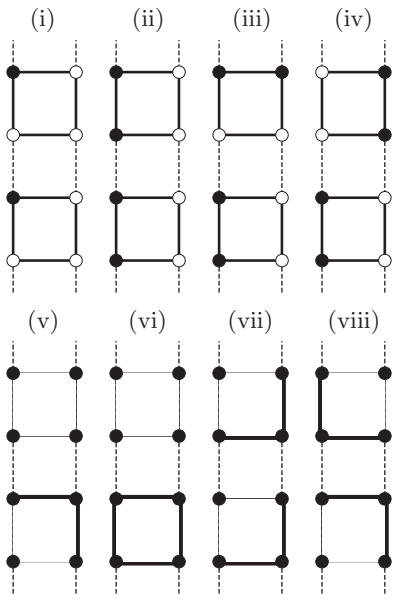

FIG. 22. Configurations of staggered on-site (i)–(iv) and bond (v)–(viii) potentials discussed in Sec. IV A. Dashed lines correspond to weak (t') bonds, solid lines correspond to strong (t) bonds, and dots correspond to lattice sites. For configurations (i)–(iv), white (black) dots correspond to on-site potential strengths $+(-)\frac{W}{2t}$. For configurations (v)–(viii), solid thin (thick) lines correspond to bond strength $1 + \frac{W}{2t}$ $(1 - \frac{W}{2t})$.

the disorder-averaged PBE, which is suppressed beyond some maximum W/t.

In the interest of brevity, we do not present data for all 32 configurations for the two types of disorder in this paper. Instead, we have identified configurations of staggered on-site potentials and hopping patterns, shown in Fig. 22, for which the pair-binding properties appear to be most robust against increasing W/t.

We observe no individual disorder configuration that enhances the PBE above its value in the clean limit for any of the disordered ladder models at any value of W/t. However, there appears to be no consistent response to increasing W/t between all configurations considered—the PBE of some configurations is suppressed rapidly as disorder increases, while the pair-binding properties of other configurations appear to be much more resistant to disorder. The maximum of the PBE for each configuration as a function of U/t and t'/t is plotted in Fig. 21.

A. Small W/t

For small W/t, the configurations (i) to (viii) in Fig. 22 lead to the largest PBEs. With the exception of configurations (i) and (vi), the staggered potentials or hoppings "pair up" locally on each plaquette, resembling a dimerlike structure. The sum of all deviations from the uniform system add to zero except for (i) and (v), with (i) and (vi) the only configurations for which the sum of the deviations do not add to zero on each plaquette.

We plot the values of Δ_p, Δ_s, and Ψ_d as a function of U/t and t'/t at doping $x = 1/8$ and $W/t = 0.25$ in Figs. 23–25 for

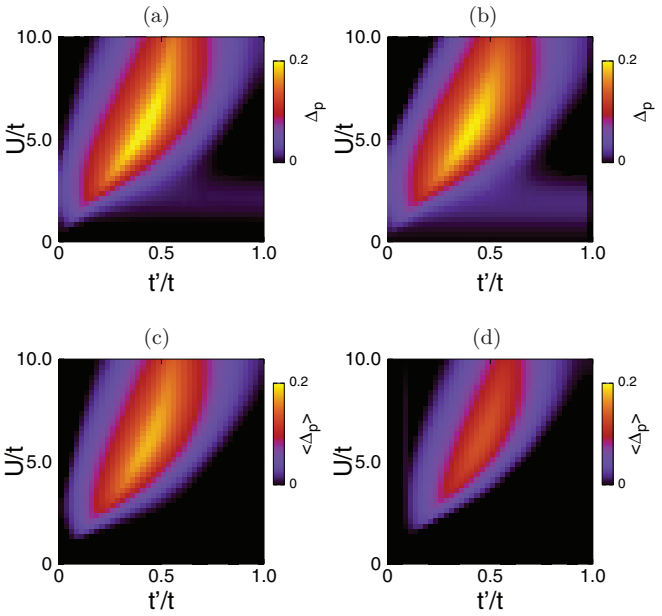

FIG. 23. (Color online) Plots of Δ_p for the eight-site ladder cluster at doping $x = 1/8$ and $W/t = 0.25$ for (a) staggered potential configuration (ii) and (b) staggered hopping configuration (vi). For comparison, we also plot $\langle\Delta_p\rangle$ at $W/t = 0.25$ for (c) potential disorder and (d) hopping disorder. (See Fig. 22 for configuration details.)

configurations (ii) and (vi) shown in Fig. 22. These data appear to be qualitatively similar to each other and to the results for other staggered configurations and for random disorder for intermediate t'/t.

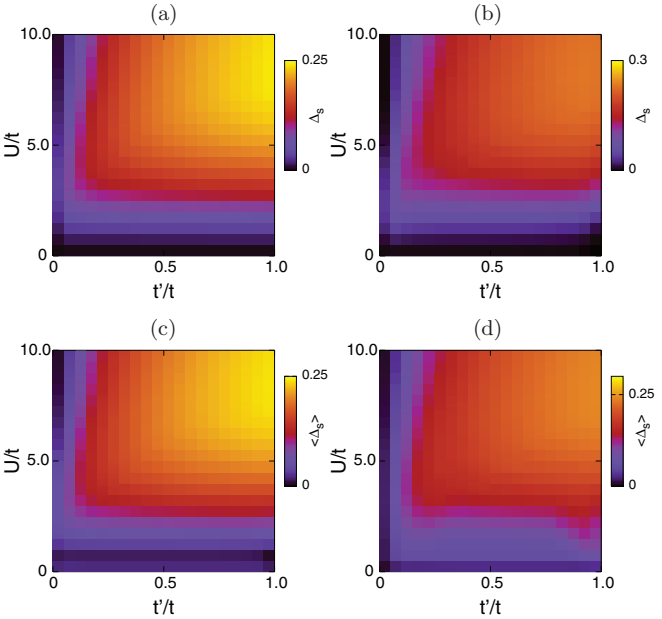

FIG. 24. (Color online) Plots of Δ_s for the eight-site ladder cluster at doping $x = 1/8$ and $W/t = 0.25$ for (a) staggered potential configuration (ii) and (b) staggered hopping configuration (vi). For comparison, we also plot $\langle\Delta_s\rangle$ at $W/t = 0.25$ for (c) potential disorder and (d) hopping disorder. (See Fig. 22 for configuration details.)

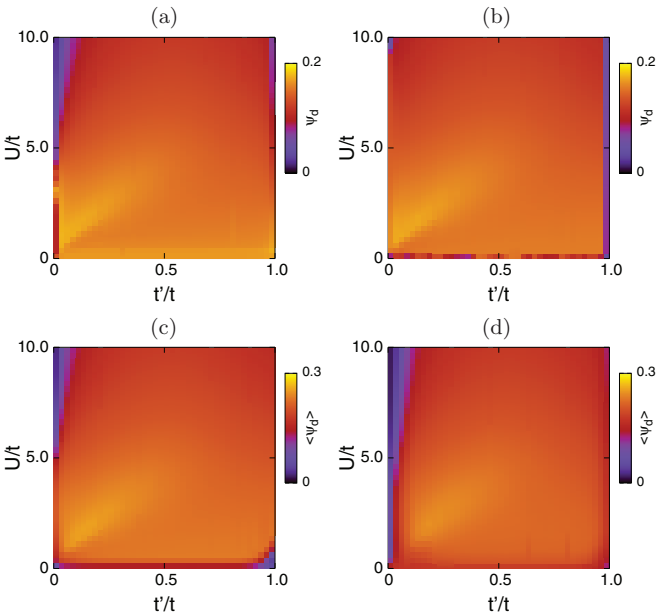

FIG. 25. (Color online) Plots of Ψ_d for the eight-site ladder cluster at doping $x = 1/8$ and $W/t = 0.25$ for (a) staggered potential configuration (ii) and (b) staggered hopping configuration (vi). For comparison, we also plot $\langle\Psi_d\rangle$ at $W/t = 0.25$ for (c) potential disorder and (d) hopping disorder. (See Fig. 22 for configuration details.)

In general, Δ_p, Δ_s, and Ψ_d appear to be the most robust against small W/t in configurations (ii)–(iv) and (vi). The local configurations of these patterns appear to favor dimerization in the case of staggered potentials and locally uniform hopping on each plaquette in the case of configuration (vi).

B. Large W/t

At large W/t Fig. 21 shows that the maxima of the PBE for configurations (I) and (II) in Fig. 26 are more robust to disorder than other configurations. Configuration (I) may be thought of as a staggered plaquette chemical potential $\mu = \pm 2W/t$, whereas configuration (II) [which is a relabelling of configuration (vi) shown in Fig. 22] may be interpreted as a hopping pattern staggered plaquette by plaquette, where the nearest neighbor hopping on each plaquette is either $t \pm W/2$.

The regions in $t' - U$ parameter space for which pair binding remains positive for large W/t are quite different for configurations (I) and (II). Pair binding is favored for

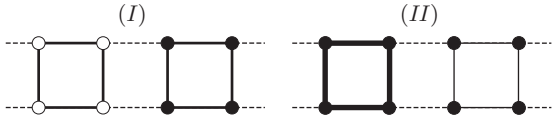

FIG. 26. Selected configurations of staggered on-site (I) and bond (II) potentials for which pair binding persists at large W/t. Dashed lines correspond to weak (t') bonds, solid lines correspond to strong (t) bonds, and dots correspond to lattice sites. For configuration (I), black (white) dots correspond to on-site potential strengths $+(-)\frac{W}{2t}$. For configuration (II), solid thick (thin) lines correspond to bond strength $1 + \frac{W}{2t}$ $(1 - \frac{W}{2t})$.

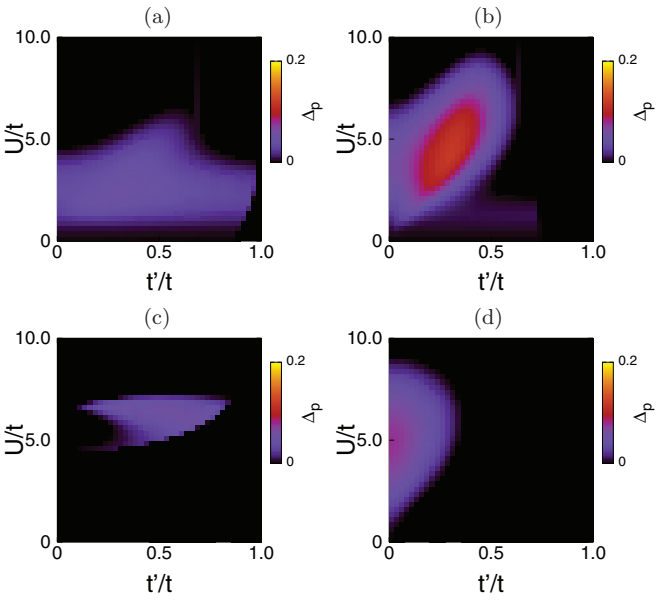

FIG. 27. (Color online) Δ_p for the eight-site ladder cluster at doping $x = 1/8$ for (a) configuration (I) at $W/t = 1.00$, (b) configuration (II) at $W/t = 1.00$, (c) configuration (I) at $W/t = 5.00$, and (d) configuration (II) at $W/t = 1.98$. (See Fig. 26 for configuration details.)

intermediate t'/t on configuration (I), whereas pair binding on configuration (II) is favored primarily as $t'/t \to 0$. For all values of W/t studied, there is always a region in parameter space where the PBE remains positive for these configurations. As shown in Fig. 27, for configuration (I), Δ_p is maximum for $t'/t \approx 0.5$ at $U/t \approx 6$–7 at $W/t = 5.00$,

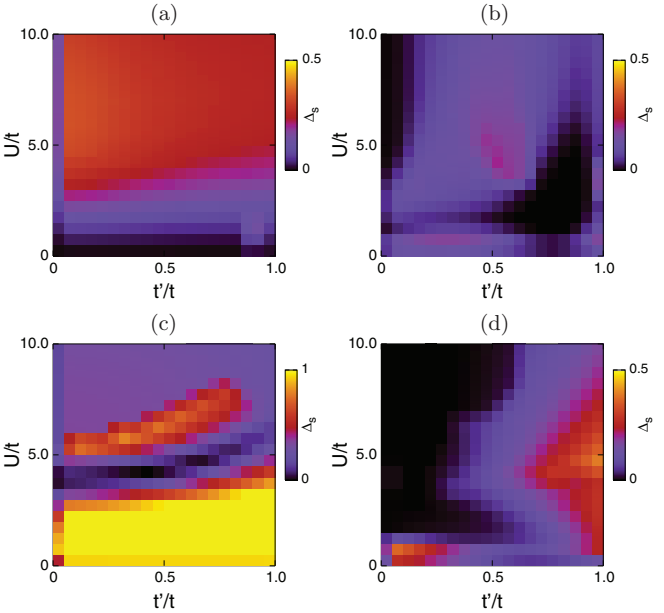

FIG. 28. (Color online) Δ_s for the eight-site ladder cluster at doping $x = 1/8$ for (a) configuration (I) at $W/t = 1.00$, (b) configuration (II) at $W/t = 1.00$, (c) configuration (I) at $W/t = 5.00$, and (d) configuration (II) at $W/t = 1.98$. (See Fig. 26 for configuration details.)

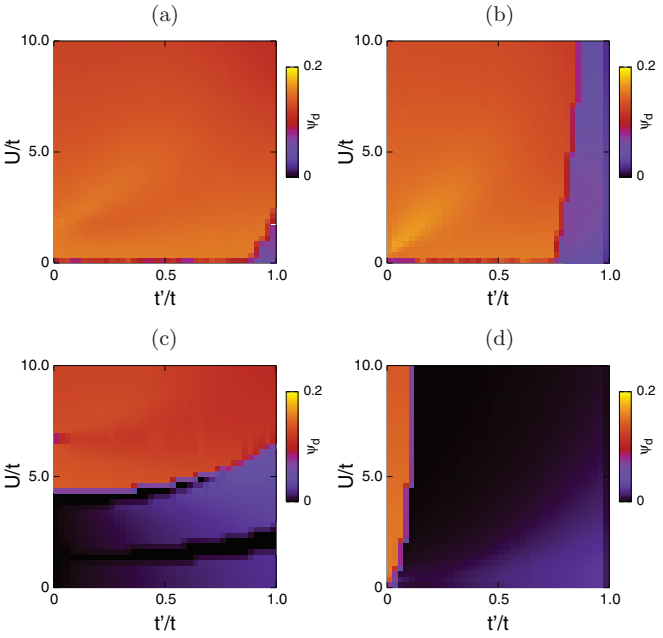

FIG. 29. (Color online) Ψ_d for the eight-site ladder cluster at doping $x = 1/8$ for (a) configuration (I) at $W/t = 1.00$, (b) configuration (II) at $W/t = 1.00$, (c) configuration (I) at $W/t = 5.00$, and (d) configuration (II) at $W/t = 1.98$. (See Fig. 26 for configuration details.)

while Δ_p is maximum along the $t'/t = 0$ axis at $W/t = 1.98$ for configuration (II).

Figures 28 and 29 show the effect of increasing W/t on the spin gap and d-wave order parameter of configurations (I) and (II) at $W/t = 1.00$ and beyond. For configuration (I), the plots of Ψ_d and Δ_s show a distinct crossover to a region where pairing is favored at $U/t \gtrsim 4$–5 at $W/t = 5.00$. For configuration (II), increasing W/t appears to shrink the spin gap in the pair-binding region, while also suppressing Ψ_d for $t'/t \gtrsim 0.1$–0.2.

For each configuration where pair binding persists for very large disorder strengths, except for the configurations shown in Fig. 26, we can identify three common characteristics. First, the maximum of Δ_p appears for intermediate U/t and $t'/t \approx 0$, which is the limit of disconnected plaquettes. Second, although the sum of all potentials across the cluster is not zero for each configuration, the values of the staggered potentials add to $\pm 2W$ on one of the plaquettes. For staggered potentials, this is tantamount to a local shift in the chemical potential of $\pm 2W$, while in the case of staggered hoppings, this is equivalent to a local change in the interplaquette hopping from $-t \to -t - W/2$. Third, the average occupation of the plaquette for which the sum of the potentials is not $\pm 2W$ is two electrons per plaquette, independent of the number of doped holes per cluster. This leaves the remaining "uniform" plaquette with four electrons per uniform plaquette at $m = 2$, five electrons per uniform plaquette at $m = 1$, and six electrons per uniform plaquette at $m = 0$.

V. DISCUSSION AND CONCLUSIONS

In this paper we have performed a detailed study of the effects of disorder on superconducting tendencies in the

checkerboard Hubbard model. From exact diagonalization studies of eight- and twelve-site ladders at dopings $x = 1/8$ and $x = 1/12$, respectively, we have found that superconducting tendencies are much more robust to disorder at moderate t'/t than for the uniform Hubbard model ($t'/t = 1$). In particular, the disorder-averaged pair-binding energy $\langle\Delta_p\rangle$, and the probability of nonzero pair-binding $P(\langle\Delta_p\rangle > 0)$ are peaked for intermediate U and t'/t and decay more slowly with disorder than for the uniform case. We observed similar behavior for $\langle\Delta_s\rangle$ and $\langle\Psi_d\rangle$. This implies a real space picture in which disorder leads to patches of superconductivity, some of which persist even to strong disorder. Such a picture emerges from studying the full distribution of pair-binding energies in the presence of disorder, not just the mean value. This additional robustness to disorder is reminiscent of the observation of stabilization of the pseudogap by disorder in Lanczos and quantum Monte Carlo simulations.[32]

Examining fluctuations in the pair-binding energy, in Sec. III D we find that these have a cusplike minimum in the region of strongest superconducting tendencies, which appears to correspond to a crossover between single-plaquette and more delocalized physics, reminiscent of the phase transition to the d-Mott state at half-filling. We note that the behavior of fluctuations in the vicinity of the maximum of the pair-binding energy is quite nonuniform and depends on the direction in the $U - t'$ plane away from the "optimal inhomogeneity." This tends to suggest that the robustness of superconducting tendencies to disorder is not just from the fact that the value of the pair-binding energy is maximum for these values of U and hence larger fluctuations are required to eliminate superconductivity. If disorder mainly modifies the position in parameter space of the localized/extended state crossover, it is this crossover that governs the maximum PBE, and hence the robustness of superconducting properties to disorder is driven by the underlying mechanism that leads to superconducting tendencies in the model rather than just the fact that the PBE is largest in this region in parameter space. (This is consistent with our observations in Sec. IV shown in Fig. 21 that for weak disorder the maximum value of the pair-binding energy is not greatly affected by staggered potentials but that the position in parameter space where that maximum is found does vary.) This picture gives an account of our results and is consistent with the plots obtained for σ_p in Figs. 19 and 20.

To gain further insight into disorder effects on the CHM, we studied all eight-site configurations in which a staggered potential or staggered hopping was superimposed on the underlying CHM. We found that the configurations with the greatest robustness to increasing disorder strength generally appeared to be those with a pattern of dimerization in either the staggered potential or hopping. A caveat to our results is the issue of finite size effects, which are always present in numerical calculations. In disordered systems, one generically expects shorter correlation lengths than the corresponding ordered system, which is encouraging. However, it would be desirable to have our results confirmed via other techniques, such as the contractor renormalization approach[9] or the dynamical cluster approximation.[11]

Beyond the focus on the two dimensional Hubbard model from the perspective of high temperature superconductivity, the interest in "designer Hamiltonians"[33–35] and the checkerboard Hubbard model in particular[21,22] in the context of cold atom systems gives an additional area to which our results may be of interest. The crossover between single plaquette and multiplaquette physics we see away from half-filling is reminiscent of the transition to the d-Mott insulator phase,[7,8,21,36] which has been argued to be favored at half-filling and is not adiabatically connected to any band insulators. In this phase each plaquette on the lattice has a local d-wave symmetry: rotation of a single plaquette by 90° leads to a change in sign of the wave function of the system. Possible experimental signatures to identify the presence of this state were suggested by Peterson *et al.*[21] Cold atom systems lack disorder, but efforts to introduce disorder using incommensurate lattices[37] and optical speckle fields[38] might allow for experimental realization of the disordered CHM.

ACKNOWLEDGMENTS

The authors thank Bill Atkinson, Igor Herbut, Wei-Fang Tsai, Xin Wan, and Rachel Wortis for helpful discussions, Martin Siegert for technical support, and Westgrid for computer resources. This work was supported by NSERC.

[1] J. G. Bednorz and K. A. Müller, Z. Phys. B **64**, 189 (1986).
[2] P. W. Anderson, Science **235**, 1196 (1987).
[3] E. Dagotto, Rev. Mod. Phys. **66**, 763 (1994); T. Maier, M. Jarrell, T. Pruschke, and M. H. Hettler, *ibid.* **77**, 1027 (2005).
[4] T. A. Maier, M. Jarrell, T. C. Schulthess, P. R. C. Kent, and J. B. White, Phys. Rev. Lett. **95**, 237001 (2005); A.-M. S. Tremblay, B. Kyung, and D. Sénéchal, Low Temp. Phys. **32**, 424 (2006) [Fiz. Nizk. Temp. **32**, 561 (2006)].
[5] W. F. Tsai and S. A. Kivelson, Phys. Rev. B **73**, 214510 (2006); **76**, 139902(E) (2007).
[6] W.-F. Tsai, H. Yao, A. Läuchli, and S. A. Kivelson, Phys. Rev. B **77**, 214502 (2008).
[7] H. Yao, W.-F. Tsai, and S. A. Kivelson, Phys. Rev. B **76**, 161104 (2007).
[8] H. Yao and S. A. Kivelson, Phys. Rev. Lett. **105**, 166402 (2010).
[9] S. Baruch and D. Orgad, Phys. Rev. B **82**, 134537 (2010).
[10] D. G. S. P. Doluweera, A. Macridin, T. A. Maier, M. Jarrell, and Th. Pruschke, Phys. Rev. B **78**, 020504(R) (2008).
[11] S. Chakraborty, D. Sénéchal, and A.-M. S. Tremblay, Phys. Rev. B **84**, 054545 (2011).
[12] Other authors have also recently studied models with hopping modulations other than the checkerboard model; see, e.g., Refs. 13–16.
[13] S. Okamoto and T. A. Maier, Phys. Rev. Lett. **101**, 156401 (2008).
[14] S. Okamoto and T. A. Maier, Phys. Rev. B **81**, 214525 (2010).
[15] S. Okamoto, D. Sénéchal, M. Civelli, and A.-M. S. Tremblay, Phys. Rev. B **82**, 180511(R) (2010).
[16] S.-Q. Su and T. A. Maier, Phys. Rev. B **84**, 220506(R) (2011).
[17] R. Schumann, Ann. Phys. (NY) **11**, 49 (2002).
[18] J. M. Tranquada, B. J. Sternlieb, J. D. Axe, Y. Nakamura, and S. Uchida, Nature (London) **375**, 561 (1995).

[19]J. E. Hoffman, E. W. Hudson, K. M. Lang, V. Madhavan, H. Eisaki, S. Uchida, and J. C. Davis, Science **295**, 466 (2002); J. E. Hoffman, K. McElroy, D.-H. Lee, K. M. Lang, H. Eisaki, S. Uchida, and J. C. Davis, *ibid.* **297**, 1148 (2002); C. Howald, H. Eisaki, N. Kaneko, M. Greven, and A. Kapitulnik, Phys. Rev. B **67**, 014533 (2003); T. Hanaguri, C. Lupien, Y. Kohsaka, D.-H. Lee, M. Azuma, M. Takano, H. Takagi, and J. C. Davis, Nature (London) **430**, 1001 (2004); M. Vershinin, S. Misra, S. Ono, Y. Abe, Y. Ando, and A. Yazdani, Science **303**, 1995 (2004); K. McElroy, D.-H. Lee, J. E. Hoffman, K. M. Lang, J. Lee, E. W. Hudson, H. Eisaki, S. Uchida, and J. C. Davis, Phys. Rev. Lett. **94**, 197005 (2005); G. Levy, M. Kugler, A. A. Manuel, O. Fischer, and M. Li, *ibid.* **95**, 257005 (2005); T. Hanaguri, Y. Kohsaka, J. C. Davis, C. Lupien, I. Yamada, M. Azuma, M. Takano, K. Ohishi, M. Ono, and H. Takagi, Nat. Phys. **3**, 865 (2007); Y. Kohsaka, C. Taylor, K. Fujita, A. Schmidt, C. Lupien, T. Hanaguri, M. Azuma, M. Takano, H. Eisaki, H. Takagi, S. Uchida, and J. C. Davis, Science **315**, 1380 (2007); W. D. Wise, M. C. Boyer, K. Chatterjee, T. Kondo, T. Takeuchi, H. Ikuta, Y. Wang, and E. W. Hudson, Nat. Phys. **4**, 696 (2008).

[20]A. Mesaros, K. Fujita, H. Eisaki, S. Uchida, J. C. Davis, S. Sachdev, J. Zaanen, M. J. Lawler, and E.-A. Kim, Science **333**, 426 (2011).

[21]M. R. Peterson, C. Zhang, S. Tewari, and S. Das Sarma, Phys. Rev. Lett. **101**, 150406 (2008).

[22]A. M. Rey, R. Sensarma, S. Fölling, M. Greiner, E. Demler, and M. D. Lukin, Europhys. Lett. **87**, 60001 (2009).

[23]A. V. Gorshkov, S. R. Manmana, G. Chen, J. Ye, E. Demler, M. D. Lukin, and A. M. Rey, Phys. Rev. Lett. **107**, 115301 (2011).

[24]K. A. Kuns, A. M. Rey, and A. V. Gorshkov, Phys. Rev. A **84**, 063639 (2011).

[25]G. Karakonstantakis, E. Berg, S. R. White, and S. A. Kivelson, Phys. Rev. B **83**, 054508 (2011).

[26]W. Cho, R. Thomale, S. Raghu, and S. A. Kivelson, arXiv:1305.2228.

[27]A. F. Kemper, D. G. S. P. Doluweera, T. A. Maier, M. Jarrell, P. J. Hirschfeld, and H.-P. Cheng, Phys. Rev. B **79**, 104502 (2009).

[28]T. A. Maier, M. S. Jarrell, and D. J. Scalapino, Phys. Rev. Lett. **96**, 047005 (2006).

[29]T. A. Maier, D. Poilblanc, and D. J. Scalapino, Phys. Rev. Lett. **100**, 237001 (2008).

[30]A. Garg, M. Randeria, and N. Trivedi, Nat. Phys. **4**, 762 (2008).

[31]W.-F. Tsai (private communication).

[32]S. Chiesa, P. B. Chakraborty, W. E. Pickett, and R. T. Scalettar, Phys. Rev. Lett. **101**, 086401 (2008).

[33]D. Jaksch, C. Bruder, J. I. Cirac, C. W. Gardiner, and P. Zoller, Phys. Rev. Lett. **81**, 3108 (1998).

[34]I. Bloch, Nat. Phys. **1**, 23 (2005).

[35]D. Jacksch and P. Zoller, Ann. Phys. (NY) **315**, 52 (2005).

[36]A. Läuchli, C. Honerkamp, and T. M. Rice, Phys. Rev. Lett. **92**, 037006 (2004).

[37]R. B. Diener, G. A. Georgakis, J. Zhong, M. Raizen, and Q. Niu, Phys. Rev. A **64**, 033416 (2001).

[38]M. White, M. Pasienski, D. McKay, S. Q. Zhou, D. Ceperley, and B. DeMarco, Phys. Rev. Lett. **102**, 055301 (2009).